SUPPLEMENTARY FIGURES AND VIDEOS

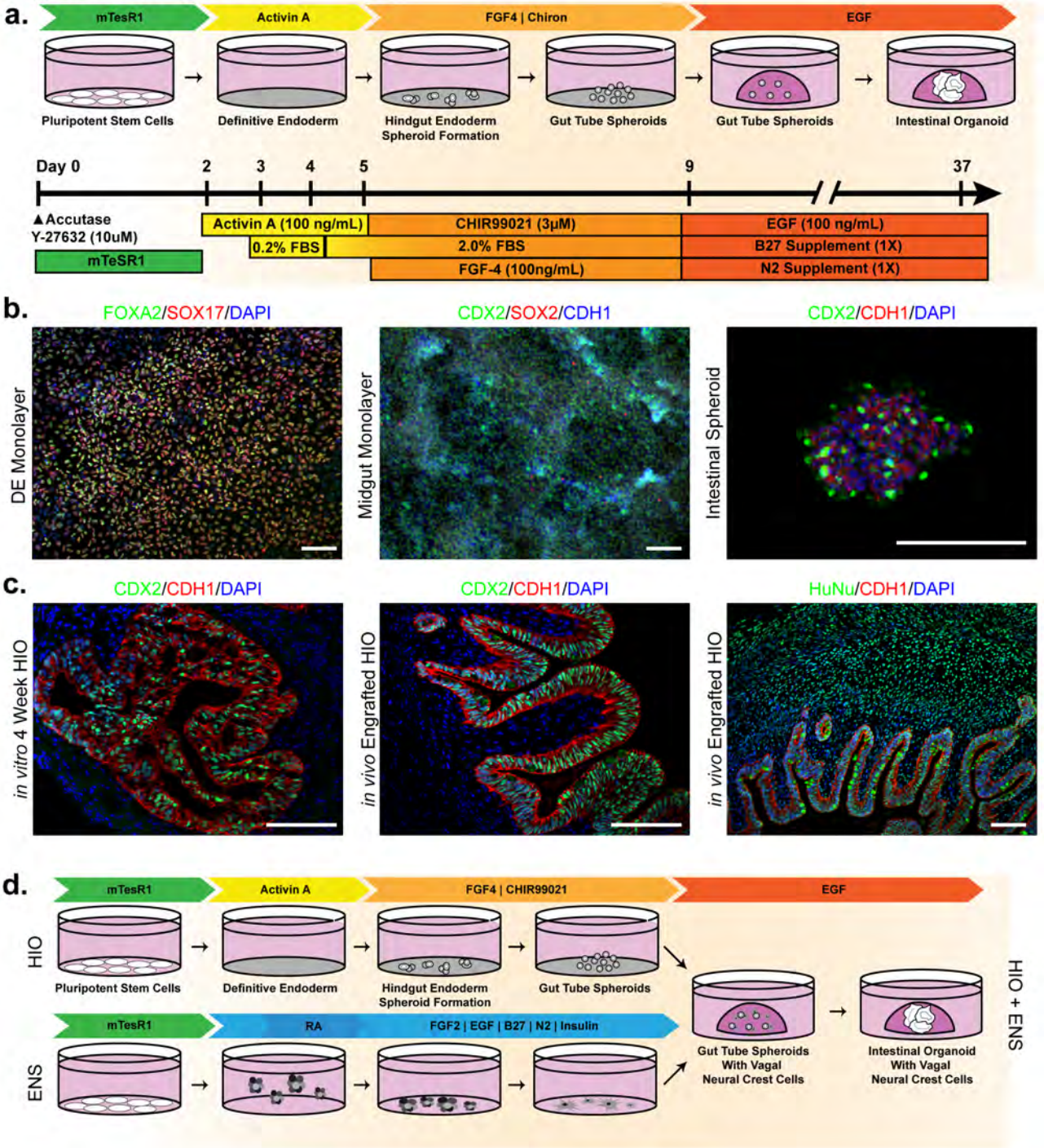

Supplementary Figure 1. Generation of Human Intestinal Organoids (HIOs). **(a)** Method for generating HIOs through directed differentiation of human pluripotent stem cells. **(b)** Temporal expression of differentiation markers at each stage of HIO development. Activin A mediated efficient differentiation into definitive endoderm

(FOXA2$^+$ and SOX17$^+$) and WNT activation in combination with FGF4 induced CDX2 expression in monolayers and free-floating spheroids. Data representative of 3 independent experiments. **(c)** Growth of spheroids in Matrigel for 4 weeks resulted in the formation of HIOs expressing CDX2$^+$ epithelium. Data representative of 6 independent experiments. HIOs were engrafted into the kidney subcapsular space of mice, where after 6 weeks they grew and matured to form intestinal tissue with crypts and villi. The human-specific antibody HuNu shows that intestinal epithelium and mesenchyme are human in origin. Data representative of 3 independent experiments. Scale bars, 100 μm **(d)** Schematic for generating and incorporating vagal NCCs into HIOs (to accompany figure 1). HIOs and NCCs are generated separately, combined by low-speed centrifugation, embedded in Matrigel and grown for 4 weeks *in vitro*.

Nature Medicine: doi:10.1038/nm.4233

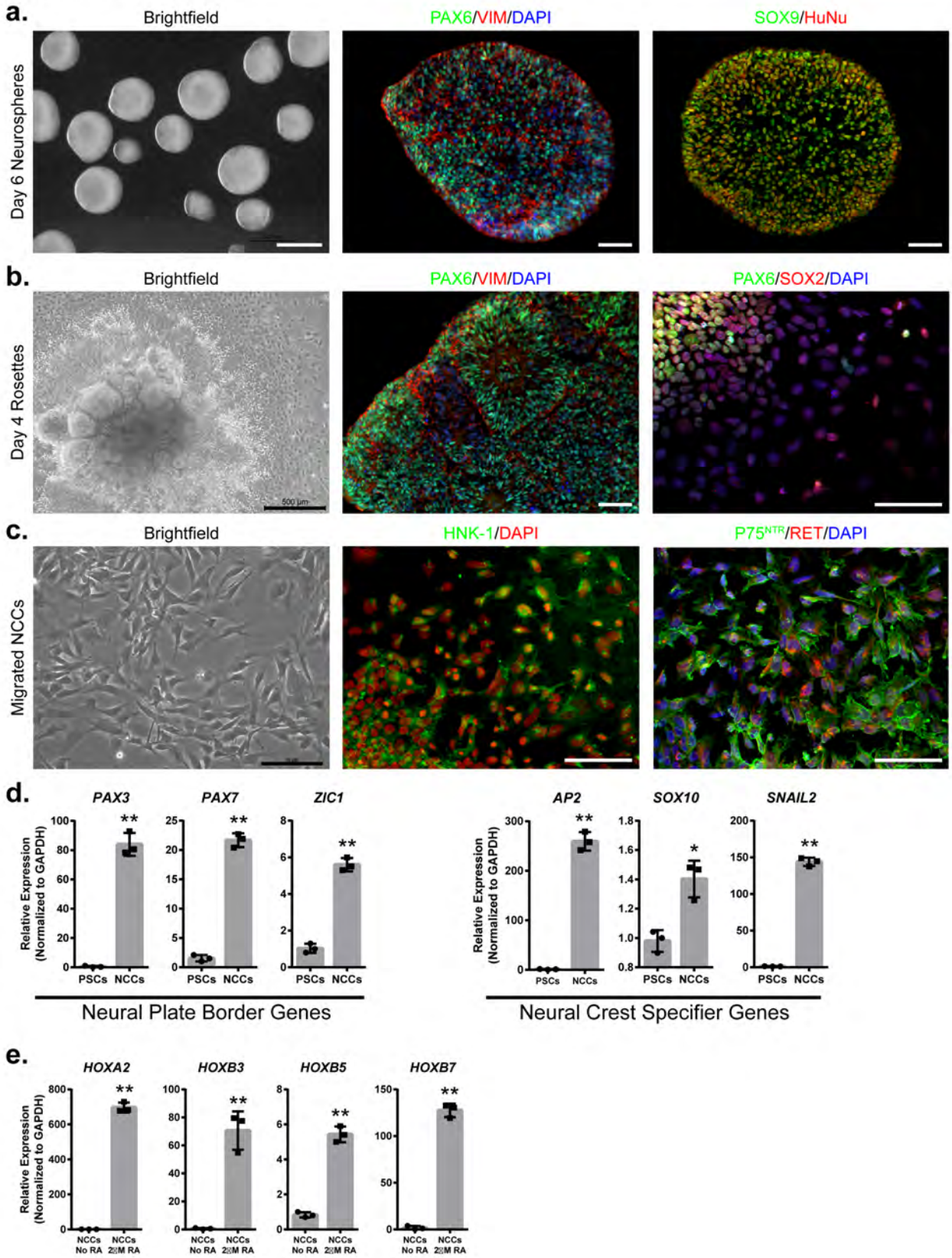

Supplementary Figure 2. Generation of vagal-like Neural Crest Cells (NCCs).

Nature Medicine: doi:10.1038/nm.4233

(a) Day 6 free-floating neurospheres are roughly 500 µm in diameter and positive for PAX6, Vimentin, and SOX9, characteristic of neural stem cells and the lateral neural plate where neural crest cells form. **(b)** Neurospheres attached to a fibronectin substrate and formed neural rosettes visible with bright field microscopy. Attached neurospheres broadly expressed PAX6 whereas Vimentin staining was observed at the edge of neural rosettes where NCCs were delaminating. As NCCs migrated away from rosettes, PAX6 was down regulated whereas SOX2 expression was maintained. Scale bars, 500 µm (left panels), 100 µm (middle and right panels). **(c)** NCCs displayed stellate morphology and were positive for surface markers HNK-1, $p75^{NTR}$, and RET. Scale bars, 50 µm (left panel), 100 µm (middle and right panels). **(d)** Quantitative RT-PCR analysis of neural plate border genes and regulators of neural crest cell specification. **(e)** Treatment of neurospheres for 48 hours with RA results in the formation of NCCs that express Vagal-level *HOX* genes. Values in graphs represent mean ± s.e.m.; * $P < 0.01$, ** $P < 0.001$; Student's *t*-test (two-tailed, unpaired); n=3 (cell culture replicates) per condition; data representative of 3 independent experiments.

Nature Medicine: doi:10.1038/nm.4233

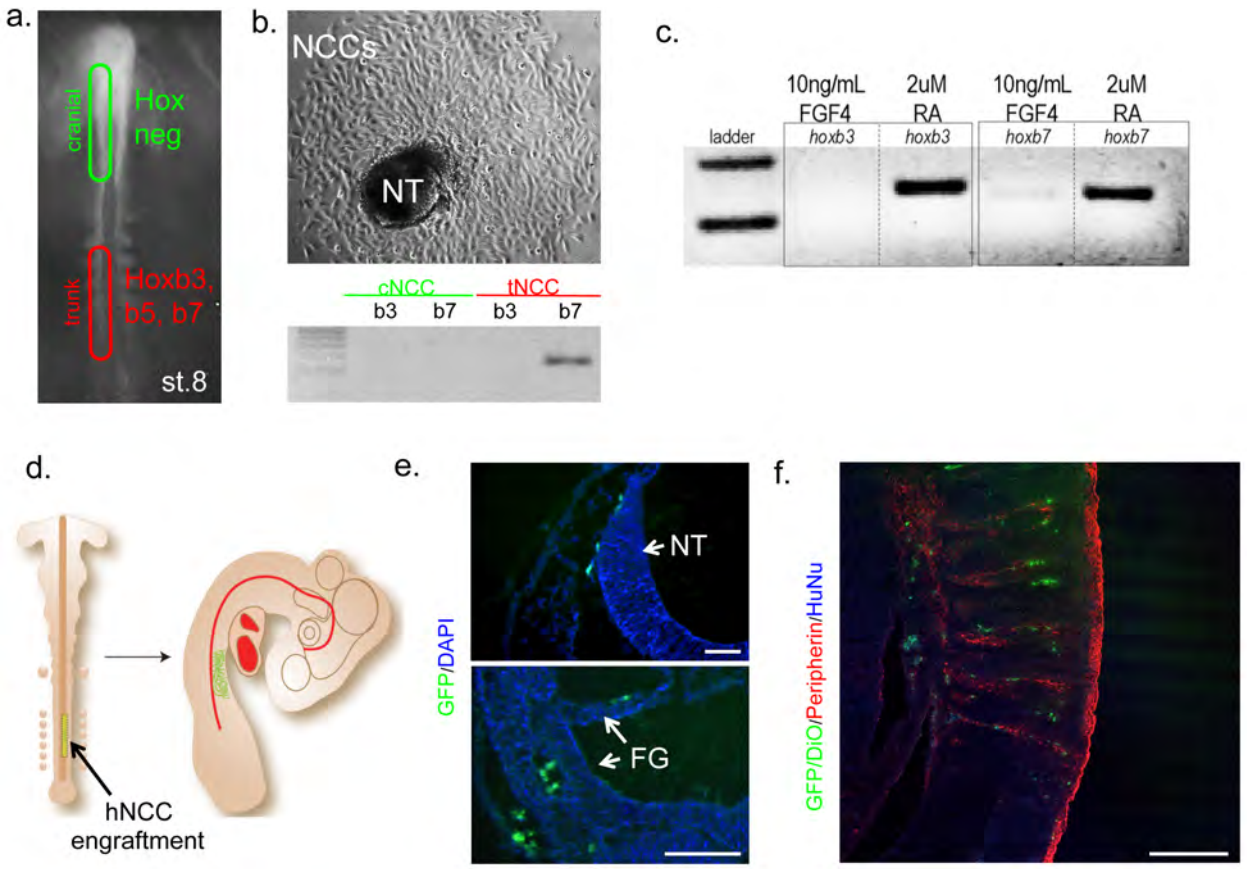

Supplementary Figure 3. Comparison of human and chick NCC behavior.
(a and b) Isolation and culturing of cranial (*Hox*-negative) and trunk (*Hox*-positive) NCCs from chick embryos and analysis of *Hox* gene expression. NCCs isolated from anterior chicken neural tube do not express *Hox* genes while those isolated from posterior neural tube are *HoxB7* positive. **(c)** Chicken cranial NCCs express vagal-level Hox genes *HoxB3* and *HoxB7* when treated with 2 µM RA for 48 hours. A different posteriorizing factor, FGF4, had no effect on *Hox* gene expression. **(d)** Schematic describing engraftment of human PSC-derived NCCs into chicken embryos. GFP-labeled human NCCs were injected intersomitically into HH10-12 chick embryos *in ovo*. **(e)** Embryos were analyzed at ~HH23. GFP-labeled cells had migrated laterally along the neural tube (NT) and could be found colonizing the foregut (FG). Scale bar, 100 µm. **(f)** Differentiation of GFP-labeled cells into peripheral neurons (Peripherin) (dorsal, right; anterior, up). Scale bar, 500 µm. Data representative of 5 independent experiments injecting human NCCs into chick embryos.

Nature Medicine: doi:10.1038/nm.4233

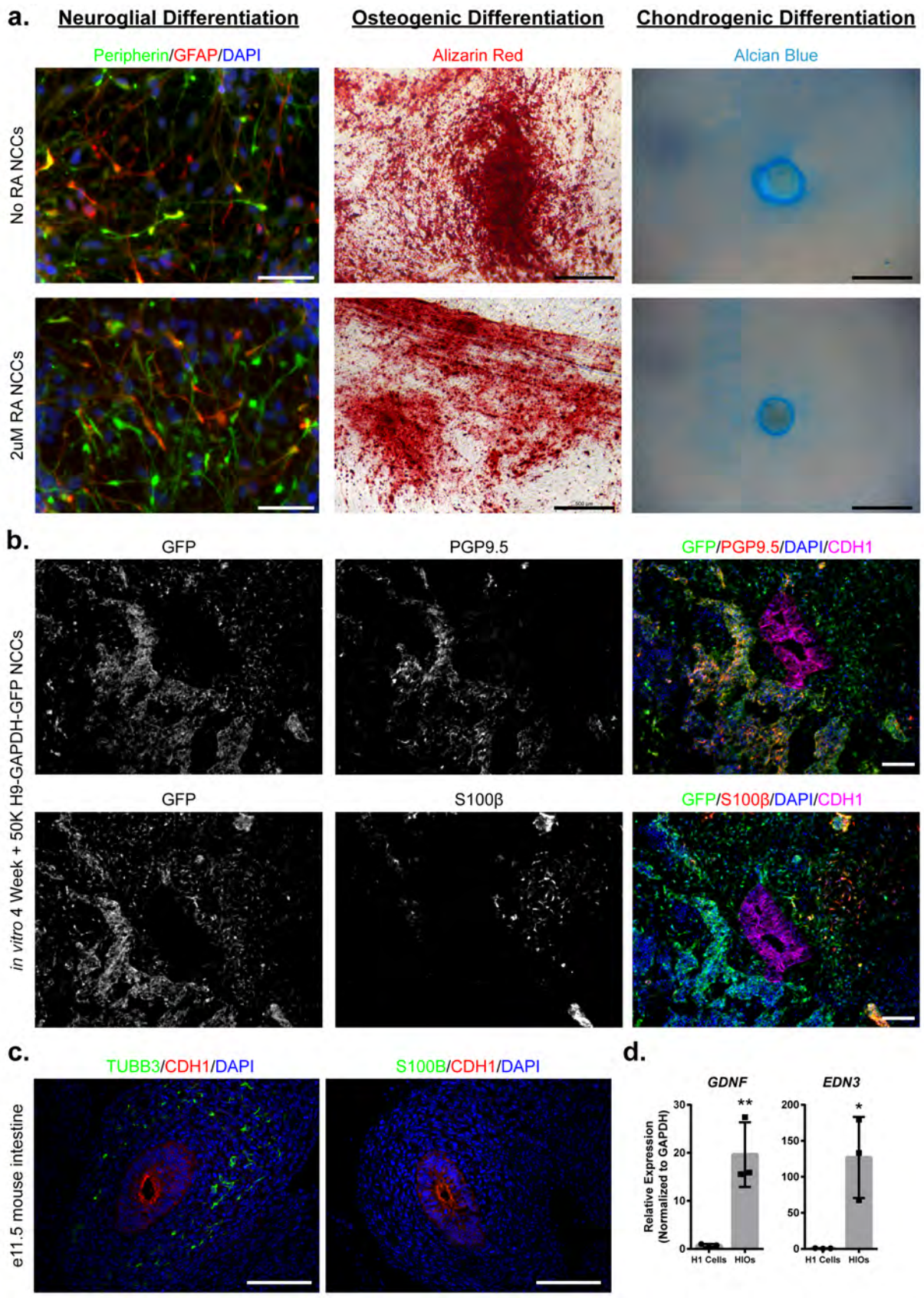

Nature Medicine: doi:10.1038/nm.4233

Supplementary Figure 4. Differentiation potential of cranial (- RA) and vagal-like (- RA) NCCs and expression of NCC migratory cues.
(a) *In vitro* differentiation of human PSC-derived NCCs into neuroglial lineages and mesenchymal lineages (osteocytes and chondrocytes). Cranial and RA-treated NCCs were equally competent to form neuroglial lineages (Peripherin and GFAP), osteocytes (alizarin red), and chondrocytes (alcian blue) *in vitro*. Scale bars, 50 μm (left panels), 500 μm (middle and right panels). Data representative of 2 independent experiments. **(b)** NCCs were generated from *H9-GAPDH*-GFP human ESCs, which ubiquitously express GFP, and combined with HIOs generated from H1 ESCs. HIOs were co-stained for GFP and pan-neuronal marker PGP9.5 or glial marker S100β. Neuroglial cells in HIOs+ENS are NCC-derived as is evidenced by co-expression of GFP and neuroglial markers. Scale bars, 100 μm. Data representative of 3 independent experiments. **(c)** Small intestine of E11.5 mouse embryo showed a similar distribution of neurons compared to HIOs+ENS *in vitro*. Although glial progenitors are present in the gut of E11.5 mouse embryos, S100β is not expressed until E14.5 suggesting that HIOs+ENS are slightly more mature than E11.5 intestine. Scale bars, 100 μm. **(d)** HIOs formed *in vitro* expressed *GDNF* and *EDN3*. Values in graphs represent mean ± s.e.m.; * $P < 0.05$, ** $P < 0.01$; *t*-test (two-tailed, unpaired); n=3 (cell culture replicates). Data are representative of 2 independent experiments.

Nature Medicine: doi:10.1038/nm.4233

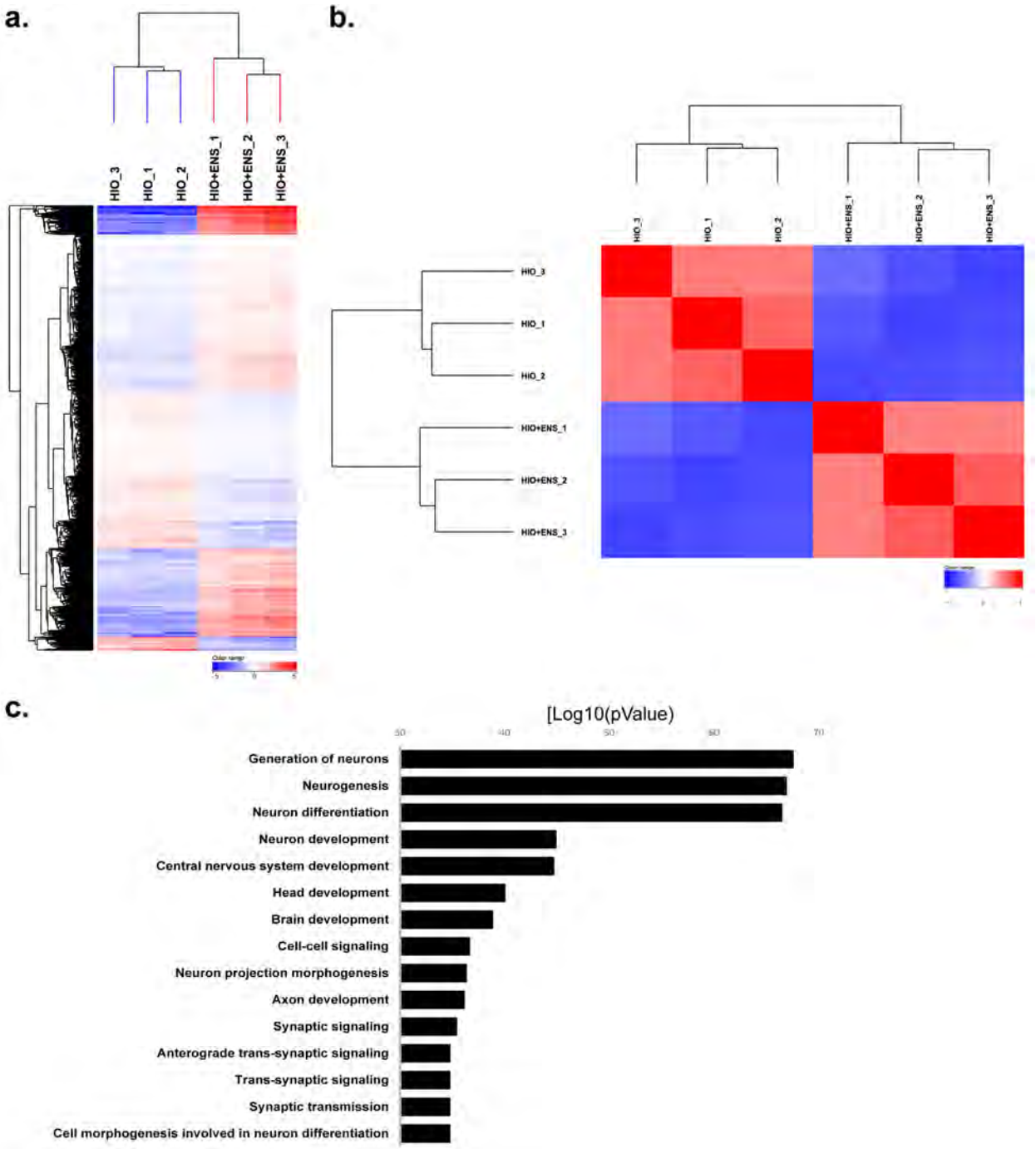

Supplementary Figure 5. Differential gene expression in HIOs+ENS *in vitro*.
(a) Heatmap was generated clustering on both gene and condition, using the Euclidean distance metric and Average linkage rule. HIOs and HIOs+ENS clustered separately according to their gene expression pattern. **(b)** Spearman correlation matrix confirmed that HIOs and HIOs+ENS presented separate and distinct cluster patterns based on gene expression. **(c)** Barplots of top 15 ontological enrichments in HIOs+ENS.

Nature Medicine: doi:10.1038/nm.4233

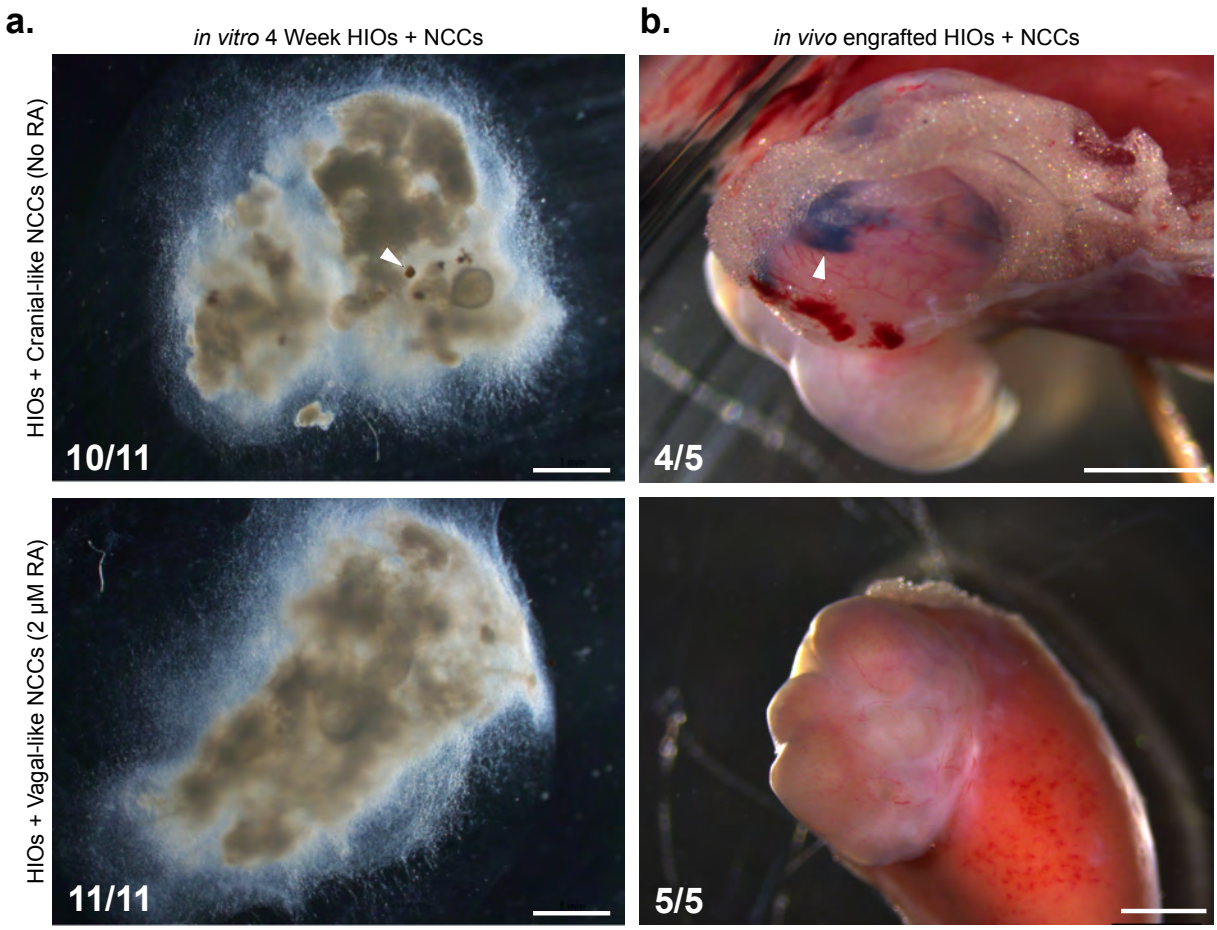

Supplementary Figure 6. HIOs + human cranial- and vagal-like NCCs engrafted *in vivo*.
(**a** and **b**) PSC-derived cranial/*HOX*-negative (no RA) and vagal/*HOX*-positive (2 µM RA) NCCs were both competent to engraft and form ENS neuroglial cells. Cranial-like NCCs formed pigmented epithelium (arrowhead) *in vitro* **(a)** and *in vivo* **(b)** suggesting a retained competence to form neuroepithelium. Scale bars, 1 mm (left panels), 2 mm (right panels)

Nature Medicine: doi:10.1038/nm.4233

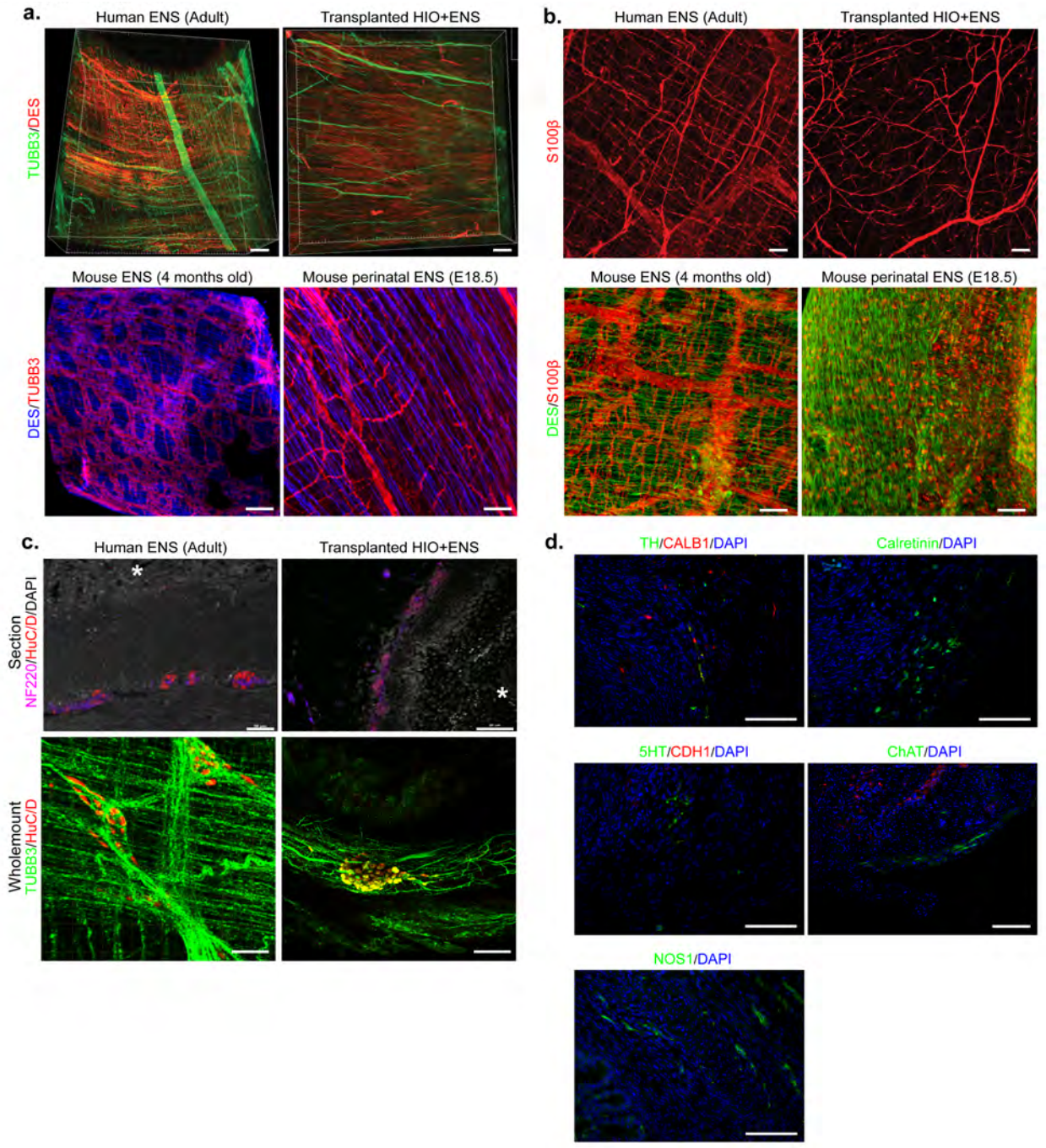

Supplementary Figure 7. HIOs+ENS grown *in vivo* form a neuroglial plexus and ganglia-like structures.
(a) Whole mount immunostaining for neurons (TUBB3, *en face* view) and muscle (DES, Desmin, *en face* view) shows neuronal network organized above the muscular layer in HIO+ENS (right panel, n=6), reminiscent of the human ENS plexus organization (left panel, n=5). Lower panel shows whole mount immunostaining of developing neurons and smooth muscle in the ENS of adult and perinatal (e18.5) mouse jejunum (n=3). Scale bars, 100 μm (upper panels), 50 μm (lower panels). **(b)** Whole mount immunostaining for glia (S100β, *en face* view) shows glial network organized similarly in

Nature Medicine: doi:10.1038/nm.4233

both human (left panel, n=5) and HIOs+ENS (right panel, n=5). Lower panel shows whole mount immunostaining of developing glia in the ENS of adult and perinatal (e18.5) mouse jejunum (n=3). Scale bar, 100 μm (upper panels), 50 μm (lower panels). **(c)** In immunostained sections (upper panels), Neurons (NF220) were spread throughout a myenteric-like plexus and contained neuronal cell bodies (HuC/D) in clusters, similar to human myenteric plexus (n=3). Scale bars, 50 μm. Whole mount (lower panel) immunostaining for neurons (TUBB3, *en face* view) and neural cell bodies (HuC/D, lateral view) shows neuronal cell bodies organized into a ganglion-like clusters in HIOs+ENS (n=5). Scale bars, 100 μm. Data representative of 3 independent experiments. **(d)** Following engraftment *in vivo*, dopaminergic neurons (TH), interneurons (ChAT, 5-HT), sensory neurons (CALB1), excitatory neurons (Calretinin) and inhibitory neurons (nNOS) were all found in HIOs+ENS. Scale bar, 100μm.

Nature Medicine: doi:10.1038/nm.4233

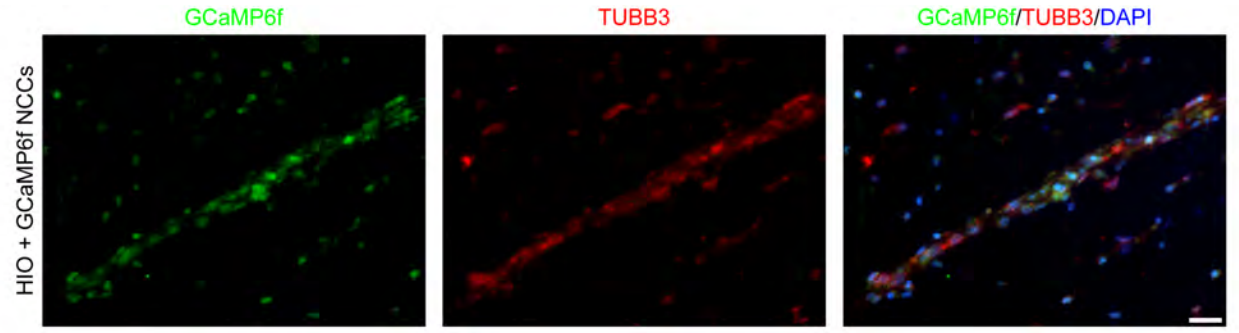

Supplementary Figure 8. Neuronal cells express GCaMP6f^{+}.
Following 28-42 days in culture, HIOs+ GCaMP6f-derived ENS were stained for GFP (GCaMP6f) and TUBB3. GFP is expressed in TUBB3+ cells suggesting that neuronal cells are expressing calcium transients**.** Scale bar, 50 µm. Data shown is a representative example from 4 independent experiments.

Nature Medicine: doi:10.1038/nm.4233

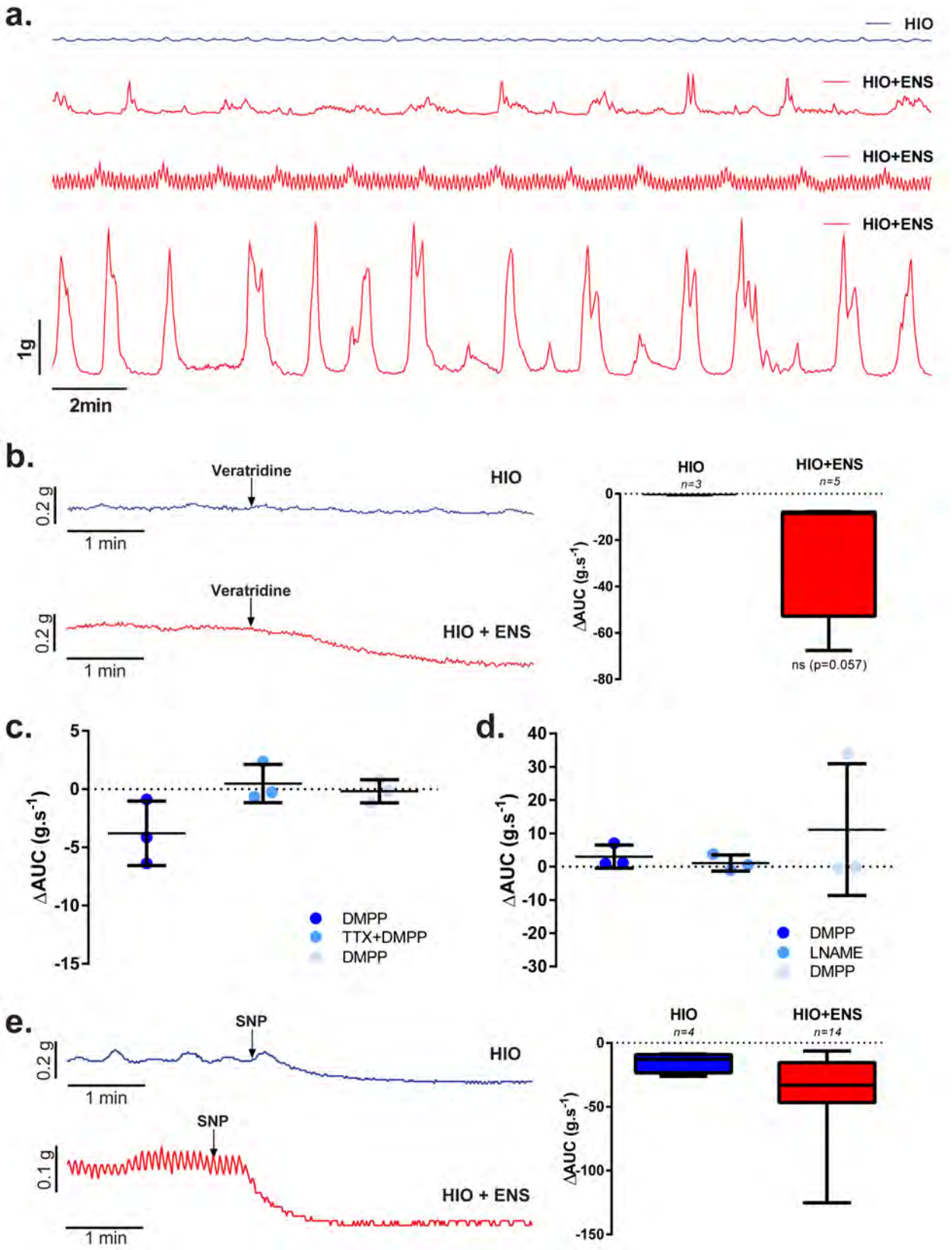

Supplementary Figure 9. Neuromuscular coupling in HIOs+ENS.

Nature Medicine: doi:10.1038/nm.4233

(a) Recordings of spontaneous contractions in transplanted HIOs and HIOs+ENS. **(b)** Left panel shows representative recording of Veratridine stimulation in HIOs (n=3) and HIOs+ENS (n=5). Right panel represents area under the curve (AUC) during Veratridine (3 μM) stimulation measured for 2 minutes before and after stimulation. **(c)** Area under the curve during Dimethylphenylpiperazinium (DMPP; 10 μM) stimulation measured for 2 minutes before and after stimulation, followed by tetrodotoxin (TTX; 10μM) treatment (n=3). **(d)** Area under the curve during DMPP stimulation measured for 2 minutes after stimulation, followed by NG-nitro-L-arginine methyl ester (L-NAME) treatment (n=3). **(e)** Left panel – representative recordings following Sodium Nitroprusside (SNP) stimulation of both HIOs (n=4) and HIO+ENS tissues (n=14). Right panel – area under the curve during SNP stimulation measured for 2 minutes before and after stimulation. Values in graphs represent mean ± s.e.m; Mann & Whitney test.

Nature Medicine: doi:10.1038/nm.4233

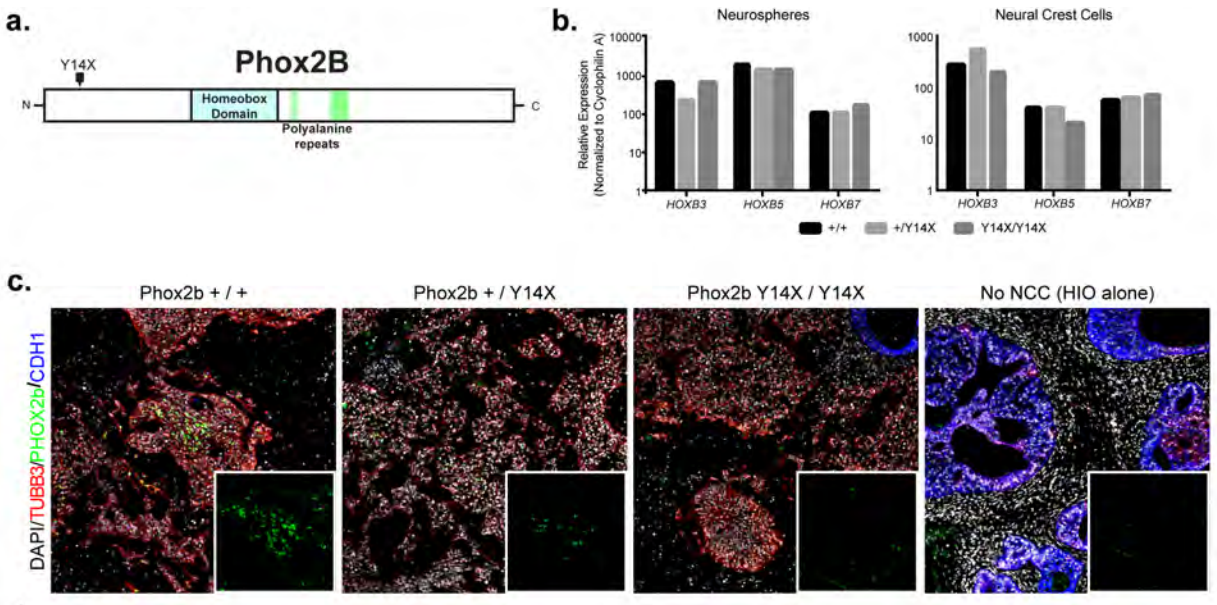

d.

Upregulated in Homo over WT		
	Source	FDR B&Y
1	forebrain regionalization	6.20E-06
2	forebrain anterior/posterior pattern specification	1.68E-04
3	forebrain dorsal/ventral pattern formation	1.95E-04
4	pattern specification process	6.00E-04
5	regionalization	6.00E-04
6	dorsal/ventral pattern formation	1.69E-03
7	forebrain neuron differentiation	3.87E-03
8	telencephalon development	4.26E-03
9	endocrine system development	4.34E-03
10	forebrain generation of neurons	4.43E-03

Downregulated in Homo over WT		
	Name	FDR B&Y
1	muscle system process	5.27E-03
2	muscle contraction	7.66E-02

Upregulated in Het over WT		
	Name	FDR B&Y
1	head development	3.84E-08
2	central nervous system development	3.84E-08
3	forebrain development	9.59E-08
4	brain development	5.08E-07
5	forebrain regionalization	2.19E-06
6	pallium development	3.67E-05
7	neuron fate commitment	3.88E-05
8	telencephalon development	7.24E-05
9	melanin biosynthetic process from tyrosine	9.00E-05
10	muscle organ development	4.73E-04

Downregulated in Het over WT		
	Name	FDR B&Y
1	epithelium development	7.78E-03
2	protein-lipid complex subunit organization	7.78E-03
3	cell adhesion	7.78E-03
4	lipoprotein localization	7.78E-03
5	lipoprotein transport	7.78E-03
6	biological adhesion	7.78E-03
7	placenta development	1.32E-02
8	tissue development	2.56E-02
9	plasma lipoprotein particle organization	2.56E-02
10	lipid transport	2.56E-02

Supplementary Figure 10. PHOX2B expression and analysis of HIOs+*PHOX2B* mutant NCCs.

(a) Schematic depicting the *PHOX2B* gene, indicating the homeobox domain and the downstream polyalanine sites. Arrow points to the targeted mutation, Y14X, present in the isogenic iPS cells used to generate neural crest cells. **(b)** Quantitative reverse-transcription PCR (qRT-PCR) data of *HOXB* genes in day 6 neurospheres and early passage neural crest cells suggesting similar patterning along the anterior-posterior axis between different *PHOX2B* genotypes at early stages. **(c)** Confocal imaging of *in vitro* cultures of HIOs±NCCs, demonstrating the absence of PHOX2B transcripts in the Y14X homozygous knockout. **(d)** Extended lists of gene ontology categories from RNA-seq analysis of expression differences in HIOs that were recombined with homozygous and heterozygous *PHOX2B* mutations compared to wild-type NCCs.

Nature Medicine: doi:10.1038/nm.4233

Supplementary Video 1. 3-dimensional image of human intestine showing enteric nerves in association with smooth muscle**.** Nerves were stained with TUBB3 (green) and smooth muscle was stained with Desmin (red). Nerves were tightly integrated into the layers of smooth muscle. Video corresponds to Supplementary Fig. 7a, top left panel.

Supplementary Video 2. 3-dimensional image of HIOs+ENS tissue grown *in vivo* showing human enteric nerves in association with smooth muscle. Nerves were stained with TUBB3 (green) and smooth muscle was stained with Desmin (red). NCC-derived nerves were embedded within the layers of smooth muscle both in the myenteric and submucosal layers. Video corresponds to Supplementary Fig. 7a, top right panel.

Supplementary Video 3. Time-lapse video of HIOs+ENS *in vitro* where the ENS was derived from neural crest cells containing a GCaMP6f reporter. Twenty-minute time-lapse video of HIOs+ENS showing Ca^{2+} flux specifically in NCC-derived cells. HIOs were generated with H1 cells, which do not have a Ca^{2+} indicator. Single neurons have regular periodicity of depolarization. Video corresponds to Supplementary Fig. 3a.

Supplementary Video 4. KCl stimulation of HIOs+ENS *in vitro*. Time-lapse video of HIOs+ENS showing broad depolarization of NCC-derived ENS cells in response to KCl addition. NCCs were generated from GCaMP6f expressing iPSCs. Video corresponds to Supplementary Fig. 3b.

Supplementary Video 5. Time-lapse video of explanted HIOs+ENS grown *in vivo* using GCaMP6f neural crest cells. A large nerve fiber was imaged where calcium oscillation was observed. NCCs were generated from GCaMP6f expressing iPSCs. Video corresponds to Fig. 3c (left panel).

Supplementary Video 6. KCl stimulation of explanted HIOs+ENS grown *in vivo* using GCaMP6f neural crest cells*.* Time-lapse video of transplanted HIOs+ENS showing depolarization of NCC-derived ENS cells in response to KCl addition. NCCs were generated from GCaMP6f expressing iPSCs. Video corresponds to Fig. 3c, right panel.

Supplementary Video 7-9. Time-lapse videos of electrically stimulated HIOs grown *in vivo*. Video 7 corresponds to the left panel of Fig. 4a (HIO) and shows an HIO lacking enteric nerves. Video 8 corresponds to the middle panel of Fig. 4a (HIO+ENS) and shows an HIO containing engrafted neural crest cells. Video 9 corresponds to the right panel of Fig. 4a (HIO+ENS) and shows an HIO containing engrafted neural crest cells that were stimulated in the presence of tetrodotoxin (HIO+ENS + TTX). Videos are played at 16X play speed.

Nature Medicine: doi:10.1038/nm.4233

TABLES

Primary Antibody	**Source**	**Dilution at RT**	**Dilution at 4C**
Goat anti-E-Cadherin	R&D #AF648		1:250
Rat anti-E-Cadherin	R&D #MAB7481		1:1000
Mouse anti-E-Cadherin	BD #610182		1:500
Rabbit anti-βIII-tubulin (TUBB3)	Abcam #ab18207		1:2000
Chicken anti-βIII-tubulin (TUBB3)	Abcam #ab41489		1:1000
Rabbit anti-c-kit/CD117 (YR145)	Abcam #ab32363		1:400
Mouse anti-HuC/D	Invitrogen #A21271		1:200
Rabbit anti-PGP9.5	Dako #Z511601		1:1000
Mouse anti-HNK-1	DSHB #1C10		1:50
Mouse anti-$p75^{NTR}$	ATS #AB-N07		1:200
Rabbit anti-Ret	Aviva #ARP30878		1:200
Goat anti-Peripherin	Santa Cruz #sc-7604		1:200
Mouse anti-GFAP	Millipore #MAB360		1:500
Rabbit anti-S100β	Dako #Z031129		1:1000
Rabbit anti-nNOS	Abcam #ab76067		1:1000
Goat anti-Desmin	Santa Cruz #sc-7559		1:100
Goat anti-Calretinin	Millipore #Ab1550		1:2000
Rabbit anti-Calbindin	Gift from K. Campbell		1:4000
Chicken anti-TH	Aves #TYH		1:500
Mouse anti-human Nuclei	Chemicon #MAB1281		1:200
Chicken anti-NF220	Ab-online #ABIN953663		1:2000
Rabbit anti-SYN1	Abcam #AB8		1:500
Mouse anti-CHGA	DHSB #CPTC-CHGA-1		1:500
Rabbit anti-CHAT	Millipore		1:200
Rabbit anti-Ki67	Thermo #RM-9106		1:500
Goat anti-GFP	Abcam #ab6673		1:200
Secondary Antibody	**Source**	**Dilution at RT**	**Dilution at 4C**
Donkey anti-mouse 488	Jackson Immuno	1:500	1:1000
Donkey anti-mouse 546	Invitrogen	1:500	1:1000
Donkey anti-goat 568	Invitrogen	1:500	1:1000
Donkey anti-rabbit 546	Invitrogen	1:500	1:1000
Donkey anti-rabbit 647	Jackson Immuno	1:500	1:1000
Donkey anti-chicken 549	Invitrogen	1:500	1:1000
Goat anti-rabbit biotin	Vector	1:500	1:1000

Horse anti-mouse biotin	Vector	1:500	1:1000

Supplementary Table 1 | Antibodies and dilutions for immunohistochemistry

Gene	**Orientation**	**Primer Sequence**
AP2α	Sense	*ATGCTTTGGAAATTGACGGA*
	Anti-sense	*ATTGACCTACAGTGCCCAGC*
Edn3	Sense	*GCACGTGCTTCACCTACAAG*
	Anti-sense	*GGACAGTCCATAGGGCACC*
GAPDH	Sense	*CCCATCACCATCTTCCAGGAG*
	Anti-sense	*CTTCTCCATGGTGGTGAAGACG*
GDNF	Sense	*TCCATGACATCATCGAACTGA*
	Anti-sense	*GTCTGCCTGGTGCTGCTC*
HoxA2	Sense	*CCAAGAAAACCGCACTTCTG*
	Anti-sense	*CATCGGCGATTTCCAGG*
HoxB3	Sense	*CGTCATGAATGGGATCTGC*
	Anti-sense	*ATATTCACATCGAGCCCCAG*
HoxB5	Sense	*GGAAGCTTCACATCAGCCAT*
	Anti-sense	*GGAACTCCTTTTCCAGCTCC*
HoxB7	Sense	*AACTTCCGGATCTACCCCTG*
	Anti-sense	*CTTTCTCCAGCTCCAGGGTC*
Pax3	Sense	*GCCGCATCCTGAGAAGTAAA*
	Anti-sense	*CTTCATCTGATTGGGGTGCT*
Pax7	Sense	*CAAACACAGCATCGACGG*
	Anti-sense	*CTTCAGTGGGAGGTCAGGTT*
Snail2	Sense	*TGACCTGTCTGCAAATGCTC*
	Anti-sense	*CAGACCCTGGTTGCTTCAA*
Sox10	Sense	*AGCTCAGCAAGACGCTGG*
	Anti-sense	*CTTTCTTGTGCTGCATACGG*

Sox9	Sense	*GTAATCCGGGTGGTCCTTCT*
	Anti-sense	*GTACCCGCACTTGCACAAC*
Zic1	Sense	*AAGATCCACAAAAGGACGCA*
	Anti-sense	*CACGTGCATGTGCTTCTTG*

Supplementary Table 2 | Primers for qPCR.